Upland forest retreat lags behind sea-level rise in the mid-Atlantic coast

Yaping Chen[1]*, Matthew L. Kirwan[1]

[1]Virginia Institute of Marine Science, William & Mary, Gloucester Point, VA, USA

* To whom correspondence and material requests should be addressed (ychen@vims.edu)

ABSTRACT

Ghost forests consisting of dead trees adjacent to marshes are striking indicators of climate change, and marsh migration into retreating coastal forests is a primary mechanism for marsh survival in the face of global sea-level rise. Models of coastal transgression typically assume inundation of a static topography and instantaneous conversion of forest to marsh with rising seas. In contrast, here we use four decades of satellite observations to show that many low-elevation forests along the US mid-Atlantic coast have survived despite undergoing relative sea-level rise rates (RSLRR) that are among the fastest on Earth. Lateral forest retreat rates were strongly mediated by topography and seawater salinity, but not directly explained by spatial variability in RSLRR, climate, or disturbance. The elevation of coastal treelines shifted upslope at rates correlated with, but far less than, contemporary RSLRR. Together, these findings suggest a multi-decadal lag between RSLRR and land conversion that implies coastal ecosystem resistance. Predictions based on instantaneous conversion of uplands to wetlands may therefore overestimate future land conversion in ways that challenge the timing of greenhouse gas fluxes and marsh creation, but also imply that the full effects of historical sea-level rise have yet to be realized.

Running head: Upland Conversion Lags Behind Sea-Level Rise

Keywords: Sea-Level Rise, Forest Mortality, Saltwater Intrusion, Lag Effect, Coastal Wetland, Marsh Migration, Climate Change

1. INTRODUCTION

Climate-driven landscape reorganization, manifested in coastal ecosystems as the migration of marshes into adjacent uplands via sea-level rise, is affecting large sections of the global coast (Kirwan & Gedan, 2019; McDowell et al., 2022; Osland et al., 2022). This phenomenon is considered one of the major processes that will fundamentally modify the feedbacks of coastal ecosystems to global climate (Chen & Kirwan, 2022a; Smart et al., 2020; Smith & Kirwan, 2021; Valentine et al., 2023; Warnell et al., 2022) and potentially incur large socio-economic repercussions (Bhattachan et al., 2018; Kirwan & Megonigal, 2013). However, predictions of coastal ecosystem transformations remain limited by an incomplete understanding of how the impacts of relative sea-level rise rate (RSLRR) are potentially mediated by spatially variable environmental drivers.

Upland forest is generally considered to be highly vulnerable to sea-level rise and saltwater intrusion (Doyle et al., 2010; Fagherazzi et al., 2019; McDowell et al., 2022). Previous estimates of coastal forest loss to sea-level rise assume that the positional change of the coastal treeline is synchronous with rising sea level (Buchanan et al., 2022; Enwright et al., 2016; Haer et al., 2013; Molino et al., 2022; Osland et al., 2022; Warnell et al., 2022). For example, recent studies based on modeled tidal datums predict that a 1.0-1.5 m mean global sea-level rise will translate into hundreds of thousands of hectares of upland forests replaced by salt marshes across the conterminous US within this century (Osland et al., 2022; Warnell et al., 2022). The resulting loss of wood production and stimulation of methane emissions contribute to a predicted net increase in the global warming potential of coastal ecosystems over large regions of the US coast (Baustian et al., 2023; Warnell et al., 2022).

However, it is unclear to what extent the predicted magnitude of forest loss will be realized, as multiple lines of evidence suggest that coastal forest retreat may not be synchronized with rising seas (Chen & Kirwan, 2022b; Schieder & Kirwan, 2019), and that other factors also play a role in modulating fine-scale patterns of coastal treeline dynamics (Fagherazzi et al., 2019; Poulter et al., 2009). For example, site-specific stratigraphic reconstructions over the past 2000 years suggest periods of time where upland conversion was slower (Schieder & Kirwan, 2019) or faster (Miller et al., 2021) than concurrent RSLRR. These reconstructions are consistent with field observations of mature trees that persist for decades under chronic flooding and salt stress (Field et al., 2016; Kirwan & Gedan, 2019; Poulter, Christensen, et al., 2008; Williams et al., 1999), and the paradigm that storms are necessary to facilitate forest retreat (Fagherazzi et al., 2019). Topography, disturbance, and biotic interactions are all factors previously invoked to interpret site-scale patterns of coastal treeline dynamics in response to rising seas (Chen & Kirwan, 2022a; Field et al., 2016; McDowell et al., 2022; Molino et al., 2022; Poulter et al., 2009; Ross et al., 1994; Schieder et al., 2018; Smith, 2013; Williams et al., 1998, 1999). Nonetheless, it is largely unknown how rates of coastal treeline retreat will manifest across broad spatial scales that stretch wide gradients of environmental context (e.g. salinity, disturbance, climate and tidal regime).

Here we leverage extensive Landsat satellite images between 1984 and 2020 to explore landscape-scale patterns, including rates and drivers of both lateral and vertical coastal treeline retreat along the US mid-Atlantic coast (Fig. 1), a global hotspot for accelerated sea-level rise (Sallenger et al., 2012). In contrast to static inundation models that assume instantaneous coastal ecosystem shifts with sea-level rise, we find that only a fraction of upland forests (~40% within elevations of 0 and 2 m) retreated inland between 1984 and 2020. Moreover, the rate of vertical forest retreat is merely half of contemporary RSLRR, pointing to a pronounced lag between sea-level rise and upland conversion that suggests surprising ecosystem resistance.

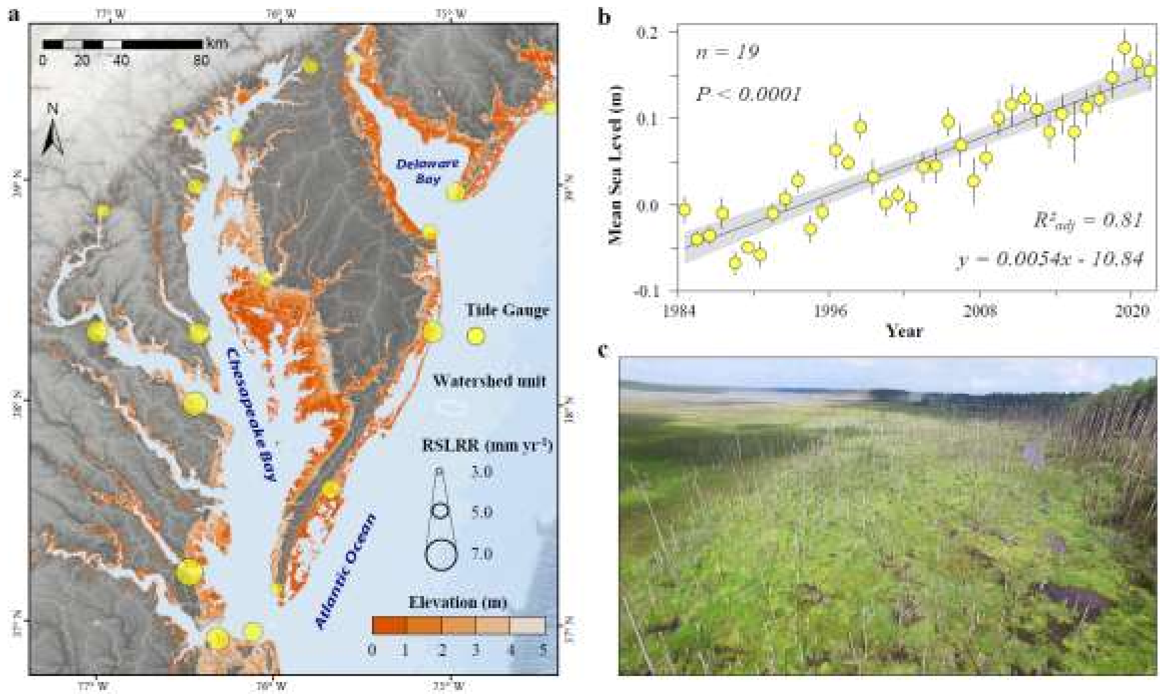

Fig. 1 | Sea-level rise along the mid-Atlantic coast of North America. **a**, Yellow circles indicate the locations of all tide gauges (*n* = 19) across the study region, where long-term information in sea level is available (1984-present). The size of the circles is proportional to the relative sea-level rise rate between 1984 and 2020. Elevation is relative to NAVD88 (mean sea level in the region). **b**, Regional sea-level rise trend averaged across all tide gauges in the region. Data shown as mean ± 1 standard deviation. The mean linear regression trendline is bounded by the 95% confidence interval. **c**, Drone image showing retreating forest in the Blackwater National Wildlife Refuge taken in 2020 (Image credit: Tyler Messerschmidt).

2. METHODS

2.1 Regional context

We studied coastal forest migration in response to sea-level rise across the US mid-Atlantic coast (~12,000 km^2; Virginia, Maryland, Delaware and New Jersey). This geophysically variable region encompasses the largest US estuary, the Chesapeake Bay, and the adjacent Delaware Bay (Fig. 1). Soil texture is relatively homogenous in the region, largely characterized as silt and silt loam (Walkinshaw et al., 2022). The region was selected because it is a known global sea-level rise hotspot (Sallenger et al., 2012), and spans strong gradients in salinity, topography, and rates of relative sea-level rise rate (RSLRR) (Table 1). Moreover, the relatively rural coast of the US mid-Atlantic represents a great opportunity to observe how sea-level driven landscape reorganization proceeds across broad scales with minimal anthropogenic obstacles (Molino et al., 2022). Indeed, massive marsh encroachment and forest mortality have been documented across the region over recent decades concurrent with increasing flooding and saltwater intrusion towards uplands (Schieder et al., 2018; Smith, 2013; White et al., 2022).

To capture the full spatial extent of sea-level rise impact (Chen & Kirwan, 2022a), we included areas between 0 and 5 m above sea level (relative to NAVD88, the mean sea level in the region) (Fig. 1). The elevation range extends from permanently flooded lowlands to coastal uplands free from seawater flooding (Pekel et al., 2016). All elevation data refers to the high precision Coastal National Elevation Database (CoNED) (Danielson et al., 2018) at 1 m resolution. All sea-level rise data are observed by long-term tidal gauges (Table 1), accessed from the NOAA Center for Operational Oceanographic Products and Services (Center for Operational Oceanographic Products and Services, 2023).

Table 1 | Sea-level rise in the US mid-Atlantic region.

Tide Gauge Station*	NOAA Code	Geolocation	Time-span	RSLRR (mm yr^{-1})	Linear regression statistics
Sewells Point, VA	8638610	36.95° N, 76.33° W	1984-2020	6.30	$R^2 = 0.82$ ($P < 0.001$)
Chesapeake Bay Bridge Tunnel, VA	8638863	36.97° N, 76.11° W	1984-2017	5.74	$R^2 = 0.79$ ($P < 0.001$)
Kiptopeke, VA	8632200	37.17° N, 75.99° W	1984-2020	4.66	$R^2 = 0.74$ ($P < 0.001$)
Yorktown, VA	8637689	37.23° N, 76.48° W	1984-2020	6.85	$R^2 = 0.86$ ($P < 0.001$)
Wachapreague, VA	8631044	37.61° N, 75.69° W	1984-2020	5.68	$R^2 = 0.79$ ($P < 0.001$)
Dahlgren, VA	8635027	38.32° N, 77.04° W	1984-2020	6.03	$R^2 = 0.83$ ($P < 0.001$)
Lewisetta, VA	8635750	37.99° N, 76.47° W	1984-2020	6.86	$R^2 = 0.84$ ($P < 0.001$)
Solomons Island, MD	8577330	38.32° N, 76.45° W	1984-2020	5.91	$R^2 = 0.86$ ($P < 0.001$)
Washington, D.C.	8594900	38.87° N, 77.02° W	1984-2020	4.84	$R^2 = 0.59$ ($P < 0.001$)
Cambridge, MD	8571892	38.57° N, 76.06° W	1984-2020	5.10	$R^2 = 0.81$ ($P < 0.001$)
Annapolis, MD	8575512	38.98° N, 76.48° W	1984-2020	5.28	$R^2 = 0.76$ ($P < 0.001$)
Baltimore, MD	8574680	39.27° N, 76.58° W	1984-2020	4.58	$R^2 = 0.76$ ($P < 0.001$)
Tolchester Beach, MD	8573364	39.21° N, 76.25° W	1987-2020	4.97	$R^2 = 0.65$ ($P < 0.001$)
Chesapeake City, MD	8573927	39.53° N, 75.81° W	1984-2020	5.13	$R^2 = 0.71$ ($P < 0.001$)
Ocean City, MD	8570283	38.33° N, 75.09° W	1984-2020	5.95	$R^2 = 0.83$ ($P < 0.001$)
Lewes, DE	8557380	38.78° N, 75.12° W	1984-2020	5.26	$R^2 = 0.80$ ($P < 0.001$)
Reedy Point, DE	8551910	39.56° N, 75.57° W	1984-2020	4.18	$R^2 = 0.72$ ($P < 0.001$)
Cape May, NJ	8536110	38.97° N, 74.96° W	1984-2020	5.81	$R^2 = 0.84$ ($P < 0.001$)
Atlantic City, NJ	8534720	39.36° N, 74.42° W	1984-2020	5.01	$R^2 = 0.75$ ($P < 0.001$)

*All sea-level data are available at the NOAA Center for Operational Oceanographic Products and Services (Center for Operational Oceanographic Products and Services, 2023). The relative sea-level rise rate (RSLRR) is computed as the slope of linear regression between year and mean sea level.

2.2 Landcover mapping

We mapped regional landcover using Landsat satellite images acquired around 1984 and 2020, and estimated lateral and vertical patterns of coastal forest retreat between 1984 and 2020 (Tables S1-S2). We did not include an intermediate time-step after taking into account the relatively slow processes of coastal forest retreat (Chen & Kirwan, 2022b; Schieder & Kirwan, 2019) combined with comparatively coarse spatial resolution of Landsat images. The extended 36-yr (1984-2020) time-span allowed us improved confidence in change detection (Chen & Kirwan, 2022a). We generated two landcover maps (one in 1984 and one in 2020 that include each of six classes: Marsh, Forest, Farmland, Urban area, Water and Sandbar, Table S1) with special focus on the marsh-forest boundary using the classification algorithm we developed earlier for accurate mapping of retreating forest in coastal landscape (Chen & Kirwan, 2022b). It is worth mentioning that 'Forest' studied here refers specifically to upland forest (Table S1), and it does not include forested wetlands (i.e. freshwater swamps). We mapped all upland forests across our study region, which stretch from higher elevations entirely devoid of seawater inundation to low-lying, salt-intruded areas at the coastal transgression front where forest species are dominated by relatively salt-tolerant evergreen trees like Loblolly pine (*Pinus taeda*) and red cedar (*Juniperus virginiana*) (Brinson et al., 1995; Kirwan et al., 2007). Both maps were created at 30 m resolution using random forest classifier in R (v. 4.1.1, packages of '*caret*' and '*randomForest*'). A detailed description of our coastal mapping approach can be found in Chen & Kirwan (2022b).

Briefly, we complemented the multispectral Landsat satellite images acquired from contrasting seasons in the year of mapping with a set of phenology metrics derived from the annual Landsat NDVI time-series for optimal differentiation between encroaching marsh and retreating forest at the upland-wetland transition (Chen & Kirwan, 2022b). For each mapping, we trained the classifier with 50% of reference sites collected earlier for different landcover types across the mid-Atlantic region (Chen & Kirwan, 2022a), and used the remaining sites for validation. All reference sites (~ 30,000) were identified according to field campaign, drone images, or high-resolution aerial images acquired in 1982-1986 (for mapping in 1984) and in 2018-2020 (for mapping in 2020) (Chen & Kirwan, 2022a), and the sites were divided randomly by landcover type in the ratio of 1:1 for training and validation.

The resulting maps were processed further for enhanced accuracy following similar post-processing steps as addressed in Chen & Kirwan (2022a). First, we assigned all areas where flooding frequency is identified by Global Surface Water dataset (1984-2020) (Pekel et al., 2016) as greater than 95% to water. Next, areas of potential misclassification of marshes were identified and removed according to the rules of flooding frequency less than 5% and elevation greater than 2.5 m (upper tidal range of mid-Atlantic (Danielson et al., 2018)). Finally, we manually digitized all areas (~5% of the study region) precluded from auto-classification due to contamination by cloud/cloud-shadow in the input Landsat images using high-resolution aerial images following the approach by Chen, Lara, et al. (2021). The final landcover maps were validated extensively across the region, which achieved an overall classification accuracy of 92.4% (*Kappa* coefficient = 0.91) and 94.5% (*Kappa* coefficient = 0.93) for the map in 1984 and 2020, respectively (Table S2).

2.3 Coastal treeline and coastal forest retreat

Using the landcover maps generated above, we then extracted coastal treelines in 1984 and 2020 following the approach of Chen & Kirwan (2022b). Coastal treelines in this study refer specifically to the marsh-forest boundary (or in less frequent occasions where coastal forests meet seawater or sandy shores as commonly seen on barrier islands) (Chen & Kirwan, 2022a, 2022b; Schieder et al., 2018; Schieder & Kirwan, 2019), and they do not include treelines where forests border human land use like farmland or urban areas, which were removed prior to analysis. To understand the spatial distribution and temporal changes of coastal treelines along topography, we systematically sampled the elevation and slope data along all coastal treelines every 100 m ('Generate Points Along Line' tool in ArcGIS v10.7) from the CoNED DEM (Danielson et al., 2018) (Fig. 2).

We differenced the landcover maps in 1984 and 2020 to identify areas of forest change, and then estimated rates of lateral and vertical forest retreat based on unique patterns of forest boundary change. The step by step methodology is illustrated in Fig. 2, modified from the framework in Chen & Kirwan (2022b) to quantify both lateral and vertical forest retreat. In brief, there are four patterns of forest loss depending on coastal treeline configuration: Interior loss (P1: emerging forest loss, treeline present only in 2020), Entire loss (P2: complete patch loss, treeline present only in 1984), Linear retreat (P3: parallel retreat with conjoint treelines in 1984 and 2020), and Radial retreat (P4: concentric retreat with disjoint treelines in 1984 and 2020) (Fig. 2). All areas of forest loss were converted to smoothed polygons ('Smooth Polygon' in ArcGIS v10.7) with the boundaries classified either as treeline in 1984 or in 2020. In general, forest losses in P1 and P2 are usually small in size, collectively accounting for less than 10% of regional forest loss, with the remaining 90% areas of forest loss roughly equally represented by P3 and P4.

Next, we generated transects running through the polygons to represent paths of forest retreat (Fig. 2). For forest loss in patterns of P3 and P4, treelines are present in both years to indicate directional retreat from 1984 to 2020. For these areas, we placed points along all polygon boundaries at regular distance (100 m), from where we created perpendicular lines ('Create Perpendicular Lines', ArcGIS v10.7) to intersect the opposite treeline (Fig. 2). Only those connecting paired treelines were selected as a retreat path, the intersection with the treeline in 1984 was determined as the start of the path, and the intersection with the treeline in 2020 was the end of the path. Unlike P3 or P4 polygons of paired treelines, the P1 and P2 polygons have a single treeline, present either in 1984 or in 2020. For each of these polygons, we generated a theoretical start (P1) or end (P2) point according to the CoNED DEM to direct the path of forest retreat. To be specific, the start point of the P1 polygon was identified as the location that has the lowest elevation within the polygon, whereas the end point of the P2 polygon referred to the location of the highest elevation within the polygon. In the same way, we generated points along boundaries of P1 and P2 polygons every 100 m, and connected these points with the start or the end point to represent directional change of forest from 1984 to 2020 (Fig. 2).

Finally, we computed the length of each path to represent the magnitude of lateral forest retreat, and estimated the elevation difference between the start and the end of the path to represent the magnitude of vertical forest retreat. We then divided the magnitude of lateral/vertical forest retreat by the years between 1984 and 2020 to calculate the rate of lateral/vertical forest retreat. To allow explicit representation of forest retreat pattern across the study region, we sampled forest retreat rate every 100 m along each path across all areas of forest loss, and rasterized the results ('Generate Tessellation', ArcGIS v10.7) to generate regional forest retreat maps at a spatial resolution of 0.075 km^2 (Hexagon grid, side length of 170 m). The value of each grid is calculated as the mean of all rate samples inside the grid, and grids outside polygons are assigned to a value of 0 as they correspond to areas of no forest change (Fig. 2).

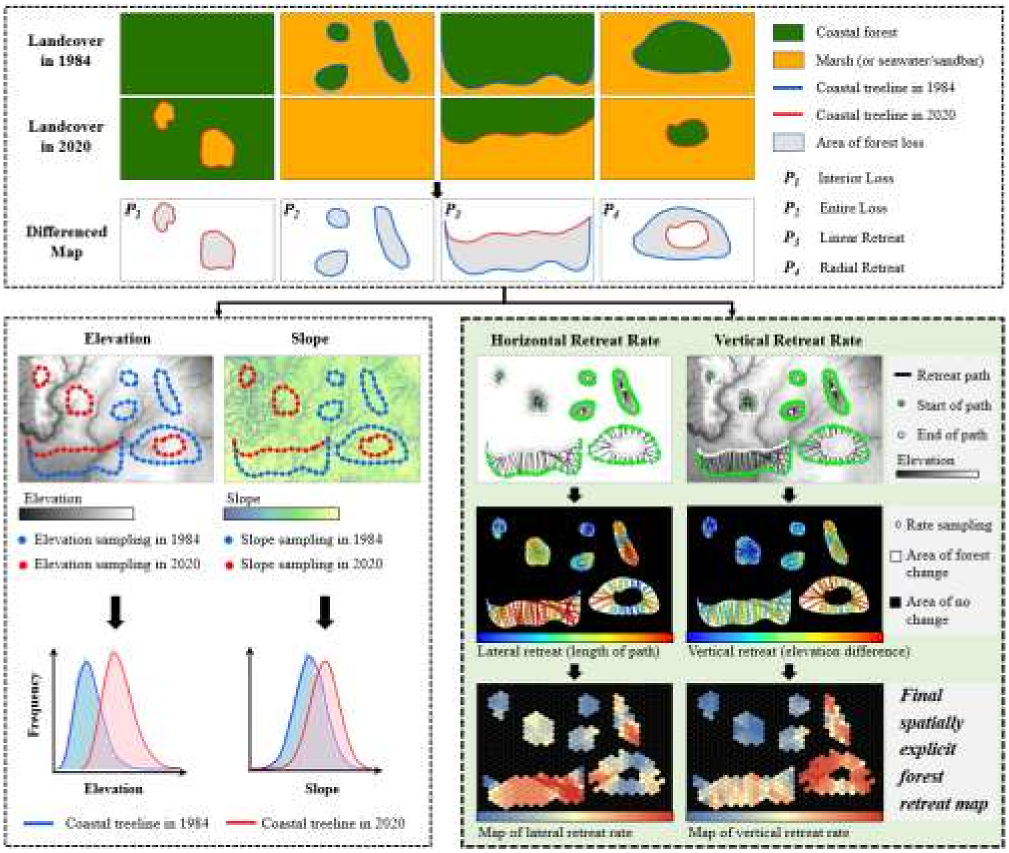

Fig. 2 | Flowchart for quantifying coastal forest retreat. The approach was modified from the framework developed in Chen & Kirwan (2022b). See Methods for detailed description of the step by step procedure.

2.4 Data analysis

We analyzed regional forest retreat rates using multiple linear regression models to identify key environmental drivers for the dynamic patterns of coastal forest change (Table 2). To explore whether the environmental controls differ between lateral and vertical forest retreat, we generated separate models for lateral retreat rate (m yr^{-1}) and vertical retreat rate (mm yr^{-1}). We fitted each model with the same set of candidate variables that includes observed RSLRR and 24 other predictors identified from literature as influential for coastal forest retreat (Table 2). Overall, these variables can be grouped into 5 broad categories: (1) climatic variables, such as precipitation, growing degree days (Chen & Kirwan, 2022a; Desantis et al., 2007; McDowell et al., 2022; White et al., 2022); (2) geophysical variables, including sea surface salinity, tidal range, and soil texture (Kirwan & Gedan, 2019; Molino et al., 2021; Schieder et al., 2018); (3) sea-level rise variables, such as RSLRR, flooding frequency (Chen & Kirwan, 2022a; Schieder & Kirwan, 2019; White &

Kaplan, 2021); (4) landscape metrics, like mean forest patch size, proximity to drainage channels (Chen, Hu, et al., 2021; Poulter, Goodall, et al., 2008; Raabe & Stumpf, 2016; Smart et al., 2020); and (5) disturbance variables, including observed storm frequency, and modeled inundation depth and duration of Hurricane Isabel (Fagherazzi et al., 2019; Ury et al., 2021; White et al., 2022).

To be consistent with sea-level rise observation, all data (except for static variables) were processed to the same time-span (1984-2020) and watershed-scale (HUC10 unit) as defined by the National Hydrography Dataset Plus (McKay et al., 2019), where the variable value of a certain watershed was computed as the mean of all forested areas within the watershed. We fitted the model with all candidate variables, and eliminated unimportant, cross-dependent/correlative variables in a stepwise manner to achieve a single reduced model that contains only significant predictors for the response variable (i.e. lateral or vertical forest retreat rate). Model performance was assessed using the adjusted coefficient of determination (R^2_{adj}), and the *Pearson*'s correlation coefficient (r) was calculated between the response variable and the set of significant predictors retained in the final model. All statistical analyses were conducted in R (v. 4.1.1) and significance was determined at the level of $p < 0.05$.

Table 2 | Candidate predictors for modeling lateral and vertical forest retreat rate. The column "Reference" refers to prior literatures suggesting relationships between coastal forest retreat and the variables selected.

Category	Variable	Description	Data source	Reference
Climatic variables	MAAT	Mean annual air temperature (ºC)	30-year normals of PRISM Climate Data ("PRISM Climate Group," 2020)	Chen & Kirwan (2022a); Desantis et al. (2007); McDowell et al. (2022); Schuerch et al. (2018); White et al. (2022)
	Tmax	Maximum air temperature (ºC)		
	TAP	Total annual precipitation (mm)		
	VPD	Maximum vapor pressure deficit (hPa)		
	GDD	Mean annual growing degree (⩾10 ºC) days	Chen & Kirwan (2022a), derived from annual PRISM Climate Data ("PRISM Climate Group," 2020)	
	ΔMAAT	Change in annual air temperature (ºC) from 1984 to 2020		
	ΔTAP	Change in annual precipitation (mm) from 1984 to 2020		
	ΔGDD	Change in annual growing degree days from 1984 to 2020		
Geophysical variables	Elevation	Elevation (meter above sea level)	CoNED DEM (Danielson et al., 2018)	Chen & Kirwan (2022a, 2022b); Chen & Ye (2014); Langston et al. (2017); Schieder et al. (2018); Smith & Kirwan (2021); Williams et al. (1998)
	Slope	Topographical slope		
	TPI	Topographic position index (unitless)		
	Aspect	Aspect (degree)		
	Salinity	Sea surface salinity (psu)	Delaware Bay (Salinity Climatology for the Mid-Atlantic, 2023); Chesapeake Bay (St-Laurent et al., 2020)	
	ST	Soil texture (unitless)	Soil properties (Walkinshaw et al., 2022)	
	R_{tidal}	Mean tide range (m), computed as the difference in height between mean high water and mean low water	NOAA Tidal Datums (NOAA Tidal Datums, 2023)	
Sea-level rise variables	FF	Flooding frequency (0-100%) between 1984 and 2020	Global Surface Water Dataset (Pekel et al., 2016)	Chen & Kirwan (2022a, 2022b); Fagherazzi et al. (2019); Schieder & Kirwan (2019)
	ΔFF	Change in flooding frequency from 1984-1999 to 2000-2020		
	RSLRR	Relative sea-level rise rate (mm yr^{-1}) between 1984 and 2020	NOAA Tides & Currents (Center for Operational Oceanographic Products and Services, 2023)	
Landscape metrics	PR	Mean proximity to channels (m)	NHDPlus Version-2 (McKay et al., 2019), and Our landcover map in 1984	Poulter, Goodall, et al. (2008); Smart et al. (2020); Ury et al. (2021)
	MPS	Mean forest patch size (m^2)		
	Compact	Mean compactness of forest patch (unitless)		
Disturbance variables	$S_{frequency}$	Number of tropical storms between 1984 and 2020	NOAA IBTrACS Project (Knapp et al., 2018)	Fagherazzi et al. (2019); Schieder & Kirwan (2019); White et al. (2022)
	$S_{severity}$	Number of hurricanes between 1984 and 2020		
	H_{depth}	Maximum inundation depth (m) by Hurricane Isabel	Storm surge simulation by ADCIRC (Molino et al., 2021)	
	$H_{duration}$	Inundation duration (h) by Hurricane Isabel		

3. RESULTS

3.1 Coastal landscape reorganization

We find that 1320.8 km^2 of the areas between 0 and 5 m NAVD88 underwent landcover change from 1984 to 2020, mostly (733 km^2) driven by human activity (e.g. deforestation), and to a lesser degree (587 km^2) by sea-level rise impacts (e.g. forest transition to marsh, Fig. 3a). However, closer examination of patterns of landcover change reveals that human-induced changes largely (67.3%) occurred at elevations greater than 2 m, whereas 96% of sea-level induced changes appeared at elevations between 0-2 m elevations (Fig. 3b). Thus, we restricted all further analysis to 0-2 m above sea level.

Within elevations between 0 and 2 m, sea-level rise impacts outpaced human activity as the predominant force responsible for over 70% of all coastal landcover change, expressed primarily as forest conversion to marsh (223.6 km^2) and marsh transition to water (171.9 km^2), followed by farmland loss to marsh and water (50.1 km^2) (Fig. 3b). In particular, sea-level driven landward marsh migration led to the creation of 257.3 km^2 of new marsh, which overcompensated marsh loss at coastal margins and resulted in an overall increase of marsh area of 78.8 km^2 from 1984 to 2020 (Fig. 3). In contrast, 235.7 km^2 of forests were deforested by rising seas from 1984 to 2020. In spite of reforestation from abandoned farmland (180.8 km^2), the total area of coastal forest decreased by 88.7 km^2 (Fig. 3b).

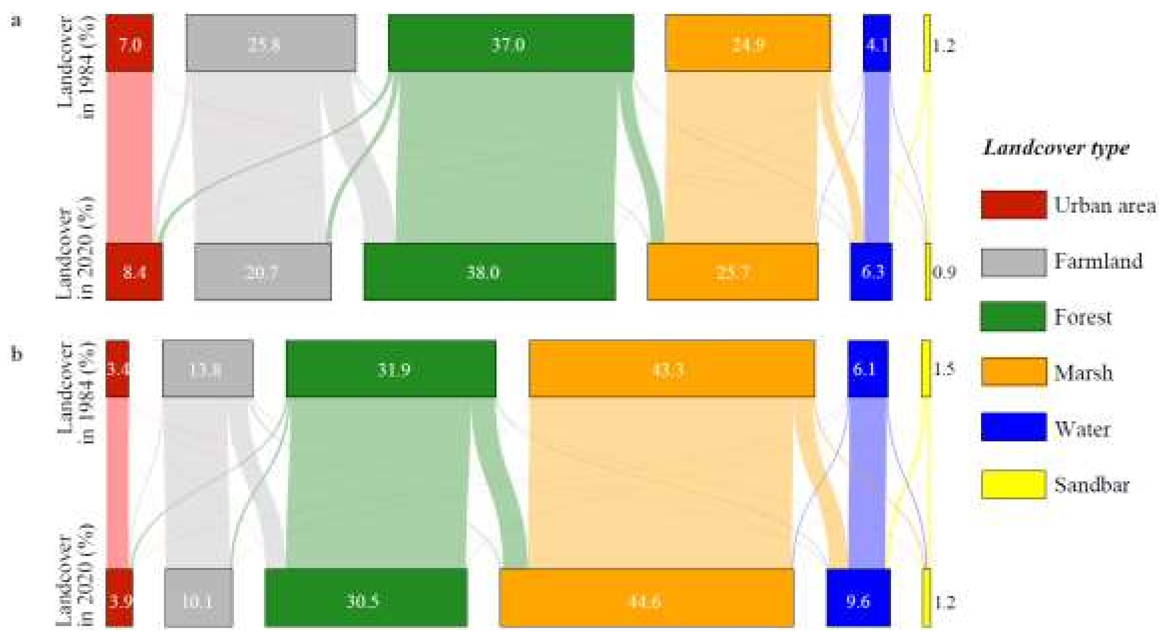

Fig. 3 | Patterns of coastal landcover change in the US mid-Atlantic region from 1984 to 2020. a, Landcover change for all areas between 0 and 5 m above sea level. **b**, Landcover change for all areas between 0 and 2 m above sea level. Alluvial plots illustrate the direction and magnitude of changes between landcover types. Numbers given indicate the percent cover of each landcover type.

3.2 Lateral forest retreat

We detect that coastal forest retreat was widespread across the mid-Atlantic region (Fig. 4 and Fig. S1), with an average lateral retreat rate of 0.67 ± 0.01 m yr^{-1} (mean ± SE) between 0 and 2 m elevations (Fig. 4a). However, not all forested areas retreated with rising seas, and the average forest retreat rate exhibited declining trends with elevation (r = -0.70, p < 0.001, Figs. 4-5). Overall, 41% of coastal forests retreated, whilst 56% of the forests remain unchanged with the remaining 3% showing treeline advance (primarily in the Virginia Coastal Reserve due to natural barrier island rollover (Deaton et al., 2017)) (Fig. 4c). The proportion of retreating forest decreased rapidly from ~70% at elevations below 0.3 m above sea level to ~10% at elevations of 1.9-2.0 m (Fig. 4c). Accordingly, lateral forest retreat rates declined from a maximal rate of 1.93 ± 0.09 m yr^{-1} at elevations of 0.2-0.3 m to 0.12 ± 0.01 m yr^{-1} at elevations of 1.9-2.0 m.

To explore the linkage between spatially-variable lateral forest retreat rate and relative sea-level rise rates (RSLRR, n = 19) observed in local watersheds, we averaged the spatially-explicit map (Fig. 4a) by watershed to generate a watershed-scale forest retreat map (Fig. 4b). Interestingly, we do not detect a statistical relationship between lateral forest retreat rate and RSLRR (p = 0.88, Fig. 4d). The lack of correlation is confirmed by our multiple linear regression model (R^2_{adj} = 0.69, $p < 0.001$, Fig. 6a), suggesting that lateral forest retreat rate is strongly and positively influenced by sea surface salinity ($p < 0.01$), and negatively influenced by elevation ($p < 0.05$) and topographical slope ($p < 0.05$). Whereas salinity emerges as the most influential variable responsible for 38.5% of the variance, topography – the combination of elevation and slope – accounts for the majority of overall variance (55.2%) in lateral forest retreat (Fig. 6a).

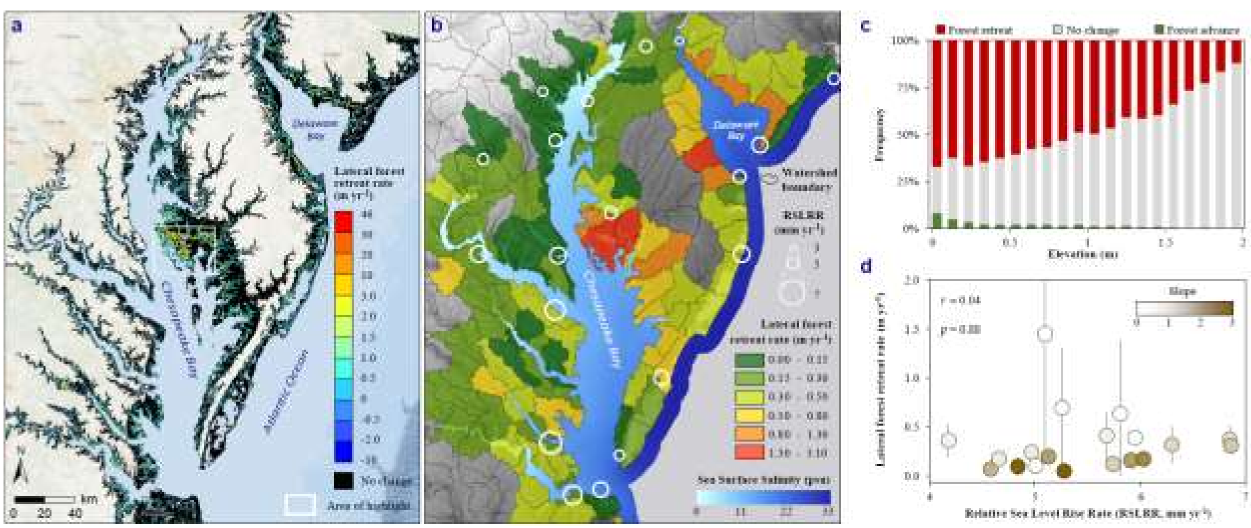

Fig. 4 | Lateral forest retreat from 1984 to 2020 across the mid-Atlantic region. a, Spatially-explicit map of lateral forest retreat rate (resolution 0.075 km^2). Positive values refer to forest retreat, and negative values represent forest advance. The white box outlines the Blackwater National Wildlife Refuge, highlighted in Fig. 5. **b**, Watershed-scale lateral forest retreat rate (HUC10 units, NHDPlus (McKay et al., 2019)). White circles refer to relative sea-level rise rate (RSLRR) recorded by long-term tide gauges in the region. **c**, Histogram showing patterns of coastal forest dynamics along elevation. **d**, No statistical relationship between lateral forest retreat and RSLRR. Data shown as mean ± 1 standard deviation.

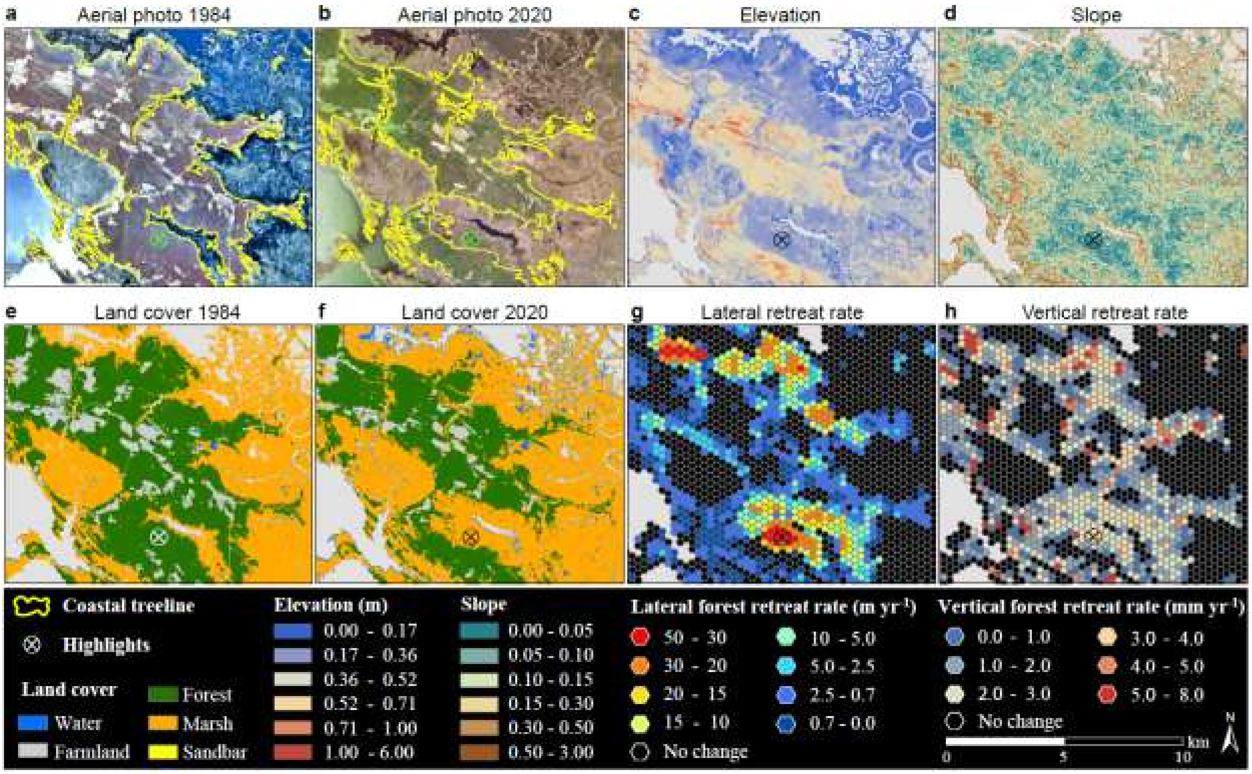

Fig. 5 | Regional subset highlighting dynamic patterns of coastal forest retreat in the Blackwater National Wildlife Refuge. High-resolution (~1.0 m) aerial photographs in 1984 (**a**) and 2020 (**b**) demonstrate variable patterns of landward marsh migration and coastal treeline retreat along gradients in elevation (**c**) and slope (**d**). The landcover maps in 1984 (**e**) and 2020 (**f**) were used to create the spatially-explicit maps of lateral (**g**) and vertical (**h**) forest retreat rate. The elevation and slope data refer to the CoNED DEM (Danielson et al., 2018).

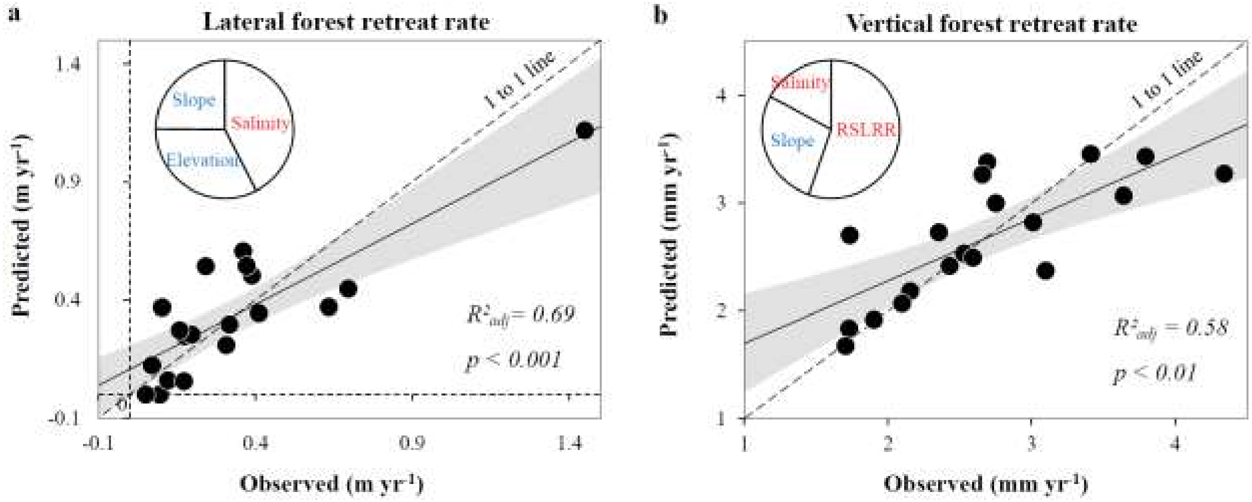

Fig. 6 | Multiple linear regression models for patterns of coastal forest retreat. Factors responsible for spatially-variable patterns of horizontal forest retreat rate (**a**) and vertical forest retreat rate (**b**). The mean linear regression trendline is bounded by the 95% confidence interval. The inserted pie charts present the relative contribution of each variable retained in the model to overall variance, where variables in red represent positive correlation with the response variable and variables in blue suggest negative correlation. RSLRR is short for relative sea-level rise rate, and salinity refers to sea surface salinity.

3.3 Vertical forest retreat

Whilst lateral forest retreat is conceptually simple, the rate is heavily influenced by terrain attributes (Figs. 4-6). To better isolate the influence of sea level on coastal forest retreat, we then created maps of vertical forest retreat (i.e. the upward migration of forest along elevation) between 1984 and 2020 (Fig. 7). Similar to patterns of lateral forest retreat, vertical forest retreat rates varied widely across the mid-Atlantic region (Fig. 7a), and declined with increasing elevation (r = -0.48, $p < 0.05$). Our multiple linear regression model suggests that RSLRR is the overriding variable ($R^2_{adj} = 0.58$, $p < 0.01$) responsible for 43.1% of the variance in vertical forest retreat (Fig. 6b). Although slope ($r = -0.51$, $p < 0.05$) and salinity ($r = 0.46$, $p < 0.05$) remain significant controls shaping the observed patterns of vertical forest retreat, they are secondary to RSLRR, explaining 21.6% and 13.3% of the variance, respectively (Fig. 6b).

Concurrent with rising sea level, the average elevation of the coastal treeline shifted upslope from 0.60 ± 0.01 m (n = 443,145) above sea level in 1984 to 0.69 ± 0.01 m (n = 468,502) above sea level in 2020 (Fig. 7c). Notably, the estimated regional mean vertical forest retreat rate of 2.71 ± 0.003 mm yr^{-1} (averaged across all forested areas between 0-2 m elevations, Fig. 7a) is less than the regional RSLRR of 5.48 ± 0.17 mm yr^{-1} (n = 19, Table 1). The deficit between forest retreat and sea-level rise is reaffirmed by the watershed-scale results (Fig. 7b). We find that although the rate of vertical forest retreat is strongly and positively correlated with RSLRR ($r = 0.55$, $p < 0.05$), the vertical forest retreat rate is merely 48.5 ± 2.6% (n = 19, range of 34.6-76.4%) of RSLRR (Fig. 7d). For instance, as RSLRR increased from 4.2 mm yr^{-1} in New Castle, Delaware to 6.9 mm yr^{-1} in Yorktown, Virginia, the corresponding vertical forest retreat rate increased from only 2.2 mm yr^{-1} to 3.8 mm yr^{-1} (Fig. 7b).

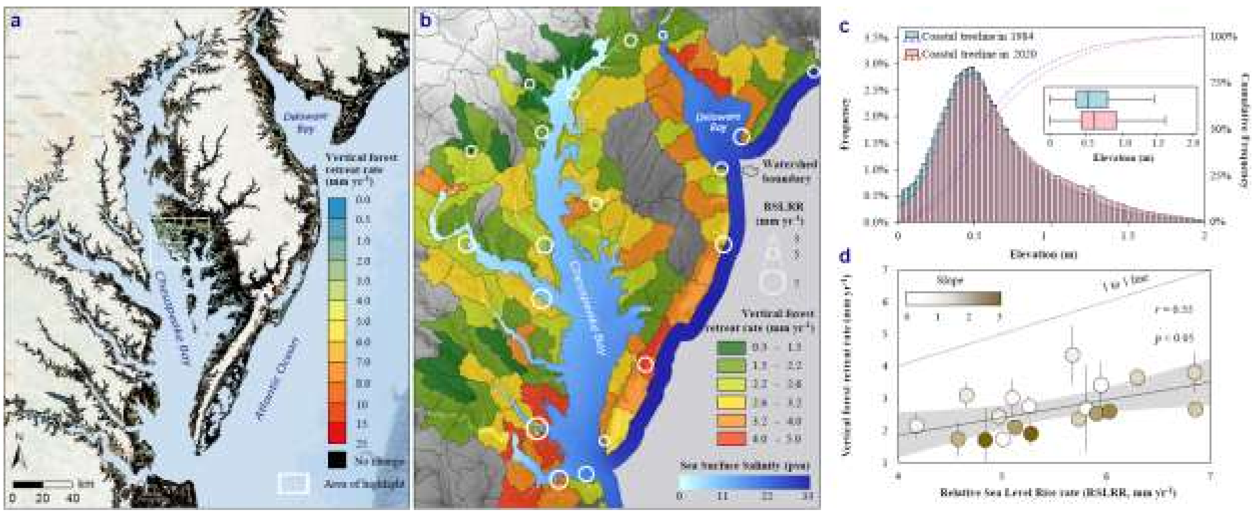

Fig. 7 | Vertical forest retreat from 1984 to 2020 across the mid-Atlantic region. **a**, Spatially-explicit map of vertical forest retreat rate (resolution 0.075 km^2). White box outlines the Blackwater National Wildlife Refuge, highlighted in Fig. 5. **b**, Watershed-scale vertical forest retreat rate (HUC10 units, NHDPlus (McKay et al., 2019)). White circles refer to relative sea-level rise rate (RSLRR) recoded by long-term tide gauges in the region. **c**, Elevation of coastal treeline shifted upslope from 1984 to 2020. The inserted panel shows the boxplot of coastal treeline elevations, where the left and right edges of the box respectively correspond to the first and third quartiles, the center line refers to the median, the white point corresponds to the mean, and the whiskers represent data within 1.5× the interquartile range. **d**, Strong positive correlation between vertical forest retreat rate and RSLRR. The dotted 1 to 1 line indicates where vertical forest retreat rate equals RSLRR. The mean linear regression trendline (solid line) is bounded by the 95% confidence interval. Data shown as mean ± 1 standard deviation.

4. DISCUSSION

4.1 Patterns and drivers of coastal forest retreat

Sea-level rise caused massive forest loss along the mid-Atlantic coast from 1984 to 2020. Notably, landward forest retreat appeared up to 10 km away from the coastline, facilitated by interconnected drainage networks. This finding complements earlier observations in coastal North Carolina (Poulter, Goodall, et al., 2008; Smart et al., 2020; Ury et al., 2021) and the Gulf of Mexico (Raabe & Stumpf, 2016), suggesting that legacy wetland management practices may serve as effective corridors for interior salinization. Nonetheless, the very condition detrimental to forest survival is conducive to inland marsh migration, which outpaced seaward marsh loss and led to an expansion of regional marsh area by 2%. Topographic and anthropogenic barriers are well known to limit marsh migration (Enwright et al., 2016; Molino et al., 2022). Interestingly, we found that with sea-level rise from 1984 to 2020, the slope at the marsh-forest boundary increased from 0.8 to 1.1, indicating that forests are retreating into progressively higher topographic slopes, which may slow marsh transgression in the future.

In spite of widespread forest loss over past decades, not all forests retreated with rising seas. In fact, only ~40% of coastal forests migrated inland between elevations of 0-2 m. Notably, stable treelines commonly occur in steeply sloped areas even at elevations in which treelines would have otherwise retreated. While it is intuitive that a gentle slope is favorable to forest migration in the lateral dimension (Chen & Kirwan, 2022a; Kirwan et al., 2016; Schieder et al., 2018; Smith, 2013), previous site-based measurements suggest contrasting relationships between topographical slope and vertical forest retreat (Fagherazzi et al., 2019; Field et al., 2016; Wasson et al., 2013). By synthesizing data across broad spatial scales, we show that both lateral and vertical forest retreat are strongly, negatively correlated with slope, highlighting steep terrain as a key asset in mediating sea-level rise impacts on adjacent uplands.

We argue that steep slopes may favor forest persistence in several ways. Aside from posing direct physical obstacles for marsh encroachment (Kirwan et al., 2016; Smith, 2013), steeper slopes generally increase the drainage area for forests downslope (Hawthorne & Miniat, 2018). Thus, forests abutting steep slopes likely receive freshwater subsidies to temper saltwater intrusion. Moreover, steep slopes minimize the distance that tree roots must extend in the landward direction to reach freshwater (Messerschmidt et al., 2021). Finally, increasing slopes also tend to shorten the duration of tidal flooding and enhance soil drainage (Hussein & Rabenhorst, 2001a, 2001b), which lessens salinization and waterlogging conditions.

Previous work suggests that increases in salinity and/or soil saturation are the primary drivers of coastal forest mortality although their effects are difficult to distinguish (McDowell et al., 2022; Smith & Kirwan, 2021). Both hypoxia and salinity are hypothesized to drive similar mechanisms of plant mortality, resulting in hydraulic failure and carbon starvation (Krauss & Duberstein, 2010; McDowell et al., 2022). The range of lateral forest retreat rates that we observed across watersheds of the mid-Atlantic coast offers empirical support to both hypotheses (Fig. 6), and it also indicates that coastal topography may interact with these processes (hypoxia, salinization) to dynamically modify the impacts of sea-level rise on coastal forest survivorship.

Interestingly, we find no relationship between rates of forest retreat and patterns of climate change or disturbance (i.e. storms), both of which are known to influence tree growth and mortality (Chen & Kirwan, 2022a; McDowell et al., 2022; Ury et al., 2021). Prior dendrochronological analyses on common coastal forest species (*Juniperus virginiana*) suggest that progressive increases in sea level suppress the impacts of climate, while strengthening the impact of tidal flooding on forest growth (Hall et al., 2022). This phenomenon potentially explains why patterns of forest retreat are not directly linked to climate, even though a warmer and wetter climate boosts forest biomass at higher elevations (Chen & Kirwan, 2022a). Similarly, although disturbance has long been regarded as important in shaping forest retreat (Fagherazzi et al., 2019; Schieder & Kirwan, 2019; Ury et al., 2021), we find no correlations between spatially-variable forest retreat and the magnitude or duration of Hurricane Isabel, the largest storm to influence the mid-Atlantic coast since the 1950s. We suspect that stochastic processes like storms may be essential in explaining coastal forest dynamics at relatively short, local scales (Walters et al., 2021), but the impacts may average out over long, broad scales – a pattern also seen in the process of barrier island retreat (Mariotti & Hein, 2022).

4.2 Lags with sea-level rise

Vertical forest retreat is strongly correlated with sea-level rise, yet the rate of vertical forest retreat is merely 35%-76% of RSLRR (Fig. 7). This result, derived from multiple decades of modern satellite observation, is supported by paleoecological evidence from sediment cores in the region, which estimated that the magnitude of vertical forest retreat (~2 m) was approximately 60%-80% that of regional sea-level rise (~2.5-3.5 m) over past millennia (Schieder & Kirwan, 2019). Both forest retreat rates and RSLRR are accelerating in the mid-Atlantic region (Chen & Kirwan, 2022b;

Ezer & Corlett, 2012; Schieder & Kirwan, 2019). However, the average vertical forest retreat rate we observed between 1984 and 2020 (2.7 mm yr^{-1}) most closely resembles the average RSLRR recorded between 1930-1950 (2.0-3.0 mm yr^{-1}) (Ezer & Corlett, 2012), implying that regional forest retreat lags behind sea-level rise by roughly half of a century. With the ever-growing power of Earth observation satellite, future studies that utilize higher spatial/temporal resolution images may help identify the precise lag and potential nonlinearities in the lag effects.

We hypothesize that a suite of internal and external mechanisms may be involved that buffer upland forests from the otherwise acute impacts of sea-level rise. For instance, greenhouse experiments reveal that tree species commonly found in coastal uplands (e.g. *Pinus taeda*, *P. serotina*) possess physiological traits allowing them to tolerate a range of flooding and low salinity conditions (Poulter, Christensen, et al., 2008; Williams et al., 1998). Recent study also indicates that coastal forests can actively adapt to rising seas through morphological plasticity, as reflected by the distribution of tree roots preferentially towards freshwater sources upslope (Messerschmidt et al., 2021). Moreover, forested wetlands in other regions accrete vertically through the accumulation of mineral sediment and organic matter (Craft, 2012; Noe et al., 2016), which may be amplified in our region by the expansion of *Phragmites australis* into transitioning forests (Langston et al., 2021).

Although forests intruded by seawater generally display reduced tree height and basal area as compared to intact forests (Krauss et al., 2009; Smith & Kirwan, 2021), remote-sensing observations and repeated field surveys suggest that many salt-intruded forests did not show biomass loss over time (Chen & Kirwan, 2022a; White & Kaplan, 2021) and some even exhibited heightened growth vigor due to enhanced light availability near forest margin (Field et al., 2016). Other factors, such as biotic interactions encouraging seedling survival (Poulter et al., 2009), the effects of marsh migration on reducing saltwater intrusion landwards (Guimond & Michael, 2021), and the capacity of coastal forests to rapidly regenerate and resprout under variable salt stress (Walters et al., 2021; Williams et al., 1998) may confer additional strength for forest persistence. Thus, although upland forests may ultimately succumb to wetlands under excessive tidal flooding, the complete transition may take years to decades to fully realize.

Our finding of a lagged response between sea-level rise and forest retreat mirrors findings in an array of terrestrial and coastal ecosystems, where sizable spatiotemporal misalignment exists between ecosystem transition and climatic forcing (Rastetter et al., 2021). For instance, the upward shifts of forest fronts in many Arctic and high-mountain regions demonstrate decadal to centennial timescale lags with climate warming (Alexander et al., 2018; Chapin & Starfield, 1997; Rastetter et al., 2021). In coastal barrier islands, the rate of barrier retreat is out of equilibrium with contemporary sea-level rise rate, but rather reflects baseline rates of past centuries (Mariotti & Hein, 2022). Similarly, marsh accretion rates lag behind accelerating sea-level rise by around 20-30 years (Kirwan & Temmerman, 2009), and marshes may persist for decades to centuries even after threshold RSLRR's are exceeded (Törnqvist et al., 2021).

Our observations of multi-decadal lags between sea-level rise and coastal forest retreat are therefore consistent with observations from a variety of earth systems responding to various facets of climate change. Numerical models of marshes, barrier islands, and terrestrial forests typically include physiological or geomorphic processes that allow ecosystems to persist under climate change until certain thresholds are surpassed (Dial et al., 2022; Kirwan & Temmerman, 2009; Mariotti & Hein, 2022). Yet, models of sea-level driven ecosystem migration are in their infancy, and typically assume that marshes migrate into adjacent uplands as soon as tidal inundation occurs (Enwright et al., 2016; Molino et al., 2022; Osland et al., 2022; Warnell et al., 2022). Incorporating newly emerging processes into numerical models are critical to predictions of coastal vulnerability and feedbacks with climate (Ward et al., 2020). In the meantime, our finding of a multi-decadal lag suggests that existing predictions based on static inundation may overestimate land conversion (Kirwan & Gedan, 2019; Osland et al., 2022), greenhouse gas emissions (Warnell et al., 2022), and marsh formation (Schuerch et al., 2018) during a given time period, but also suggests that the effects of historical sea-level rise have yet to be fully realized.

Acknowledgments. Primary funding for this work comes from the National Science Foundation (no. 1654374, 1832221 and 2012670, M.L.K.) with additional support from the US Department of Energy, Office of Biological and Environmental Research Program (DE-SC0021112, M.L.K.), U.S. Geological Survey Climate Research and Development Program and the U.S. Geological Survey Coastal and Marine Hazards and Resources Program, and National Natural Science Fund for Excellent Young Scientists Fund Program (Overseas) (Y.C.). We thank Tyler Messerschmidt and Alex Smith for their assistance in field validation, and acknowledge Kendall Valentine Cole for her feedback on the methodology. We appreciate the generosity of Marjy Friedrichs and Pierre St-Laurent for providing the salinity model output, Grace Molino for curating the tidal range dataset, and Alfredo Aretxabaleta for navigating the ADCIRC Prediction System to provide the Hurricane Isabel product.

Author Contributions. Y.C. designed the study, performed the analysis and wrote the initial draft. M.L.K contributed to the study design and revised the manuscript. Both authors interpreted the data.

Competing Interests. The authors declare no competing interest.

Data Availability. All data will be available in the Virginia Coast Reserve Long-Term Ecological Research repository.

References

Alexander, J. M., Chalmandrier, L., Lenoir, J., Burgess, T. I., Essl, F., Haider, S., Kueffer, C., McDougall, K., Milbau, A., Nuñez, M. A., Pauchard, A., Rabitsch, W., Rew, L. J., Sanders, N. J., & Pellissier, L. (2018). Lags in the response of mountain plant communities to climate change. *Global Change Biology*, *24*(2), 563–579. https://doi.org/10.1111/gcb.13976

Baustian, M. M., Liu, B., Moss, L. C., Dausman, A., & Pahl, J. W. (2023). Climate change mitigation potential of Louisiana's coastal area: Current estimates and future projections. *Ecological Applications*. https://doi.org/10.1002/eap.2847

Bhattachan, A., Jurjonas, M. D., Moody, A. C., Morris, P. R., Sanchez, G. M., Smart, L. S., Taillie, P. J., Emanuel, R. E., & Seekamp, E. L. (2018). Sea level rise impacts on rural coastal social-ecological systems and the implications for decision making. *Environmental Science & Policy*, *90*, 122–134. https://doi.org/10.1016/j.envsci.2018.10.006

Brinson, M. M., Christian, R. R., & Blum, L. K. (1995). Multiple States in the Sea-Level Induced Transition from Terrestrial Forest to Estuary. *Estuaries*, *18*(4), 648. https://doi.org/10.2307/1352383

Buchanan, M. K., Kulp, S., & Strauss, B. (2022). Resilience of U.S. coastal wetlands to accelerating sea level rise. *Environmental Research Communications*, *4*(6), 061001. https://doi.org/10.1088/2515-7620/ac6eef

Center for Operational Oceanographic Products and Services. (2023). *NOAA Tides & Currents*. National Oceanic and Atmospheric Administration. https://tidesandcurrents.noaa.gov/sltrends/

CHAPIN, F. S., & STARFIELD, A. M. (1997). TIME LAGS AND NOVEL ECOSYSTEMS IN RESPONSE TO TRANSIENT CLIMATIC CHANGE IN ARCTIC ALASKA. *Climatic Change*, *35*(4), 449–461. https://doi.org/10.1023/A:1005337705025

Chen, Y., Hu, F. S., & Lara, M. J. (2021). Divergent shrub-cover responses driven by climate, wildfire, and permafrost interactions in Arctic tundra ecosystems. *Global Change Biology*, *27*(3), 652–663. https://doi.org/10.1111/gcb.15451

Chen, Y., & Kirwan, M. L. (2022a). Climate-driven decoupling of wetland and upland biomass trends on the mid-Atlantic coast. *Nature Geoscience*. https://doi.org/10.1038/s41561-022-01041-x

Chen, Y., & Kirwan, M. L. (2022b). A phenology- and trend-based approach for accurate mapping of sea-level driven coastal forest retreat. *Remote Sensing of Environment*, *281*, 113229. https://doi.org/10.1016/j.rse.2022.113229

Chen, Y., Lara, M. J., Jones, B. M., Frost, G. V., & Hu, F. S. (2021). Thermokarst acceleration in Arctic tundra driven by climate change and fire disturbance. *One Earth*, *4*(12), 1718–1729. https://doi.org/10.1016/j.oneear.2021.11.011

Chen, Y., & Ye, Y. (2014). Effects of Salinity and Nutrient Addition on Mangrove Excoecaria agallocha. *PLoS ONE*, *9*(4), e93337. https://doi.org/10.1371/journal.pone.0093337

Craft, C. B. (2012). Tidal freshwater forest accretion does not keep pace with sea level rise. *Global Change Biology*, *18*(12), 3615–3623. https://doi.org/10.1111/gcb.12009

Danielson, J. J., Poppenga, S. K., Tyler, D. J., Palaseanu-Lovejoy, M., & Gesch, D. B. (2018). Coastal National

Elevation Database. In *Fact Sheet*. https://doi.org/10.3133/fs20183037

Deaton, C. D., Hein, C. J., & Kirwan, M. L. (2017). Barrier island migration dominates ecogeomorphic feedbacks and drives salt marsh loss along the Virginia Atlantic Coast, USA. *Geology*, *45*(2), 123–126. https://doi.org/10.1130/G38459.1

Desantis, L. R. G., Bhotika, S., Williams, K., & Putz, F. E. (2007). Sea-level rise and drought interactions accelerate forest decline on the Gulf Coast of Florida, USA. *Global Change Biology*, *13*(11), 2349–2360. https://doi.org/10.1111/j.1365-2486.2007.01440.x

Dial, R. J., Maher, C. T., Hewitt, R. E., & Sullivan, P. F. (2022). Sufficient conditions for rapid range expansion of a boreal conifer. *Nature*, *608*(7923), 546–551. https://doi.org/10.1038/s41586-022-05093-2

Doyle, T. W., Krauss, K. W., Conner, W. H., & From, A. S. (2010). Predicting the retreat and migration of tidal forests along the northern Gulf of Mexico under sea-level rise. *Forest Ecology and Management*, *259*(4), 770–777. https://doi.org/10.1016/j.foreco.2009.10.023

Enwright, N. M., Griffith, K. T., & Osland, M. J. (2016). Barriers to and opportunities for landward migration of coastal wetlands with sea-level rise. *Frontiers in Ecology and the Environment*, *14*(6), 307–316. https://doi.org/10.1002/fee.1282

Ezer, T., & Corlett, W. B. (2012). Is sea level rise accelerating in the Chesapeake Bay? A demonstration of a novel new approach for analyzing sea level data. *Geophysical Research Letters*, *39*(19), n/a-n/a. https://doi.org/10.1029/2012GL053435

Fagherazzi, S., Anisfeld, S. C., Blum, L. K., Long, E. V., Feagin, R. A., Fernandes, A., Kearney, W. S., & Williams, K. (2019). Sea Level Rise and the Dynamics of the Marsh-Upland Boundary. *Frontiers in Environmental Science*, *7*. https://doi.org/10.3389/fenvs.2019.00025

Field, C. R., Gjerdrum, C., & Elphick, C. S. (2016). Forest resistance to sea-level rise prevents landward migration of tidal marsh. *Biological Conservation*, *201*, 363–369. https://doi.org/10.1016/j.biocon.2016.07.035

Guimond, J. A., & Michael, H. A. (2021). Effects of Marsh Migration on Flooding, Saltwater Intrusion, and Crop Yield in Coastal Agricultural Land Subject to Storm Surge Inundation. *Water Resources Research*, *57*(2). https://doi.org/10.1029/2020WR028326

Haer, T., Kalnay, E., Kearney, M., & Moll, H. (2013). Relative sea-level rise and the conterminous United States: Consequences of potential land inundation in terms of population at risk and GDP loss. *Global Environmental Change*, *23*(6), 1627–1636. https://doi.org/10.1016/j.gloenvcha.2013.09.005

Hall, S., Stotts, S., & Haaf, L. (2022). Influence of Climate and Coastal Flooding on Eastern Red Cedar Growth along a Marsh-Forest Ecotone. *Forests*, *13*(6), 862. https://doi.org/10.3390/f13060862

Hawthorne, S., & Miniat, C. F. (2018). Topography may mitigate drought effects on vegetation along a hillslope gradient. *Ecohydrology*, *11*(1). https://doi.org/10.1002/eco.1825

Hussein, A. H., & Rabenhorst, M. C. (2001a). Tidal Inundation of Transgressive Coastal Areas. *Soil Science Society of America Journal*, *65*(2), 536–544. https://doi.org/10.2136/sssaj2001.652536x

Hussein, A. H., & Rabenhorst, M. C. (2001b). Modeling the Impact of Tidal Inundation on Submerging Coastal Landscapes of the Chesapeake Bay. *Soil Science Society of America Journal*, *65*(3), 932–941.

https://doi.org/10.2136/sssaj2001.653932x

Kirwan, M. L., & Gedan, K. B. (2019). Sea-level driven land conversion and the formation of ghost forests. *Nature Climate Change*, *9*(6), 450–457. https://doi.org/10.1038/s41558-019-0488-7

Kirwan, M. L., Kirwan, J. L., & Copenheaver, C. A. (2007). Dynamics of an estuarine forest and its response to rising sea level. *Journal of Coastal Research*, *23*(2), 457–463. https://doi.org/10.2112/04-0211.1

Kirwan, M. L., & Megonigal, J. P. (2013). Tidal wetland stability in the face of human impacts and sea-level rise. *Nature*, *504*(7478), 53–60. https://doi.org/10.1038/nature12856

Kirwan, M. L., Temmerman, S., Skeehan, E. E., Guntenspergen, G. R., & Fagherazzi, S. (2016). Overestimation of marsh vulnerability to sea level rise. *Nature Climate Change*, *6*(3), 253–260. https://doi.org/10.1038/nclimate2909

Kirwan, M., & Temmerman, S. (2009). Coastal marsh response to historical and future sea-level acceleration. *Quaternary Science Reviews*, *28*(17–18), 1801–1808. https://doi.org/10.1016/j.quascirev.2009.02.022

Knapp, K. R., Diamond, H. J., Kossin, J. P., Kruk, M. C., & Schreck, C. J. I. (2018). *International Best Track Archive for Climate Stewardship (IBTrACS) Project, Version 4*. NOAA National Centers for Environmental Information. https://doi.org/10.25921/82ty-9e16

Krauss, K. W., & Duberstein, J. A. (2010). Sapflow and water use of freshwater wetland trees exposed to saltwater incursion in a tidally influenced South Carolina watershed. *Canadian Journal of Forest Research*, *40*(3), 525–535. https://doi.org/10.1139/X09-204

Krauss, K. W., Duberstein, J. A., Doyle, T. W., Conner, W. H., Day, R. H., Inabinette, L. W., & Whitbeck, J. L. (2009). Site condition, structure, and growth of baldcypress along tidal/non-tidal salinity gradients. *Wetlands*, *29*(2), 505–519. https://doi.org/10.1672/08-77.1

Langston, A. K., Coleman, D. J., Jung, N. W., Shawler, J. L., Smith, A. J., Williams, B. L., Wittyngham, S. S., Chambers, R. M., Perry, J. E., & Kirwan, M. L. (2021). The Effect of Marsh Age on Ecosystem Function in a Rapidly Transgressing Marsh. *Ecosystems*. https://doi.org/10.1007/s10021-021-00652-6

Langston, A. K., Kaplan, D. A., & Putz, F. E. (2017). A casualty of climate change? Loss of freshwater forest islands on Florida's Gulf Coast. *Global Change Biology*, *23*(12), 5383–5397. https://doi.org/10.1111/gcb.13805

Mariotti, G., & Hein, C. J. (2022). Lag in response of coastal barrier-island retreat to sea-level rise. *Nature Geoscience*, *15*(8), 633–638. https://doi.org/10.1038/s41561-022-00980-9

McDowell, N. G., Ball, M., Bond-Lamberty, B., Kirwan, M. L., Krauss, K. W., Megonigal, J. P., Mencuccini, M., Ward, N. D., Weintraub, M. N., & Bailey, V. (2022). Processes and mechanisms of coastal woody-plant mortality. *Global Change Biology*, *28*(20), 5881–5900. https://doi.org/10.1111/gcb.16297

McKay, L., Bondelid, T., Dewald, T., Johnston, J., Moore, R., & Rea, A. (2019). *NHDPlus Version 2: User Guide (Data Model Version 2.1)*. 182. https://s3.amazonaws.com/nhdplus/NHDPlusV21/Documentation/NHDPlusV2_User_Guide.pdf%0Aftp://ftp.horizon-systems.com/NHDplus/NHDPlusV21/Documentation/NHDPlusV2_User_Guide.pdf

Messerschmidt, T. C., Langston, A. K., & Kirwan, M. L. (2021). Asymmetric root distributions reveal press–pulse

responses in retreating coastal forests. *Ecology*, *102*(10). https://doi.org/10.1002/ecy.3468
Miller, C. B., Rodriguez, A. B., & Bost, M. C. (2021). Sea-level rise, localized subsidence, and increased storminess promote saltmarsh transgression across low-gradient upland areas. *Quaternary Science Reviews*, *265*, 107000. https://doi.org/10.1016/j.quascirev.2021.107000
Molino, G. D., Carr, J. A., Ganju, N. K., & Kirwan, M. L. (2022). Variability in marsh migration potential determined by topographic rather than anthropogenic constraints in the Chesapeake Bay region. *Limnology and Oceanography Letters*. https://doi.org/10.1002/lol2.10262
Molino, G. D., Defne, Z., Aretxabaleta, A. L., Ganju, N. K., & Carr, J. A. (2021). Quantifying Slopes as a Driver of Forest to Marsh Conversion Using Geospatial Techniques: Application to Chesapeake Bay Coastal-Plain, United States. *Frontiers in Environmental Science*, *9*. https://doi.org/10.3389/fenvs.2021.616319
NOAA Tidal Datums. (2023). *Vertical Datum Transformation, Integrating America's Elevation Data*. NOAA/NOS's VDatum. https://vdatum.noaa.gov/download.php
Noe, G. B., Hupp, C. R., Bernhardt, C. E., & Krauss, K. W. (2016). Contemporary Deposition and Long-Term Accumulation of Sediment and Nutrients by Tidal Freshwater Forested Wetlands Impacted by Sea Level Rise. *Estuaries and Coasts*, *39*(4), 1006–1019. https://doi.org/10.1007/s12237-016-0066-4
Osland, M. J., Chivoiu, B., Enwright, N. M., Thorne, K. M., Guntenspergen, G. R., Grace, J. B., Dale, L. L., Brooks, W., Herold, N., Day, J. W., Sklar, F. H., & Swarzenzki, C. M. (2022). Migration and transformation of coastal wetlands in response to rising seas. *Science Advances*, *8*(26). https://doi.org/10.1126/sciadv.abo5174
Pekel, J.-F., Cottam, A., Gorelick, N., & Belward, A. S. (2016). High-resolution mapping of global surface water and its long-term changes. *Nature*, *540*(7633), 418–422. https://doi.org/10.1038/nature20584
Poulter, B., Christensen, N. L., & Qian, S. S. (2008). Tolerance of Pinus taeda and Pinus serotina to low salinity and flooding: Implications for equilibrium vegetation dynamics. *Journal of Vegetation Science*, *19*(1), 15–22. https://doi.org/10.3170/2007-8-18410
Poulter, B., Goodall, J. L., & Halpin, P. N. (2008). Applications of network analysis for adaptive management of artificial drainage systems in landscapes vulnerable to sea level rise. *Journal of Hydrology*, *357*(3–4), 207–217. https://doi.org/10.1016/j.jhydrol.2008.05.022
Poulter, B., Qian, S. S., & Christensen, N. L. (2009). Determinants of coastal treeline and the role of abiotic and biotic interactions. *Plant Ecology*, *202*(1), 55–66. https://doi.org/10.1007/s11258-008-9465-3
PRISM Climate Group. (2020). *Oregon State University*. http://prism.oregonstate.edu
Raabe, E. A., & Stumpf, R. P. (2016). Expansion of Tidal Marsh in Response to Sea-Level Rise: Gulf Coast of Florida, USA. *Estuaries and Coasts*, *39*(1), 145–157. https://doi.org/10.1007/s12237-015-9974-y
Rastetter, E. B., Ohman, M. D., Elliott, K. J., Rehage, J. S., Rivera-Monroy, V. H., Boucek, R. E., Castañeda-Moya, E., Danielson, T. M., Gough, L., Groffman, P. M., Jackson, C. R., Miniat, C. F., & Shaver, G. R. (2021). Time lags: insights from the U.S. Long Term Ecological Research Network. *Ecosphere*, *12*(5). https://doi.org/10.1002/ecs2.3431
Ross, M. S., O'Brien, J. J., & da Silveira Lobo Sternberg, L. (1994). Sea-Level Rise and the Reduction in Pine Forests in the Florida Keys. *Ecological Applications*, *4*(1), 144–156. https://doi.org/10.2307/1942124

Salinity Climatology for the Mid-Atlantic. (2023). Oceanic Information Center. Ocean Bytes. https://www.oceanbytes.org/2011/11/21/predicting-sea-surface-salinity-from-space/

Sallenger, A. H., Doran, K. S., & Howd, P. A. (2012). Hotspot of accelerated sea-level rise on the Atlantic coast of North America. *Nature Climate Change*, *2*(12), 884–888. https://doi.org/10.1038/nclimate1597

Schieder, N. W., & Kirwan, M. L. (2019). Sea-level driven acceleration in coastal forest retreat. *Geology*, *47*(12), 1151–1155. https://doi.org/10.1130/G46607.1

Schieder, N. W., Walters, D. C., & Kirwan, M. L. (2018). Massive Upland to Wetland Conversion Compensated for Historical Marsh Loss in Chesapeake Bay, USA. *Estuaries and Coasts*, *41*(4), 940–951. https://doi.org/10.1007/s12237-017-0336-9

Schuerch, M., Spencer, T., Temmerman, S., Kirwan, M. L., Wolff, C., Lincke, D., McOwen, C. J., Pickering, M. D., Reef, R., Vafeidis, A. T., Hinkel, J., Nicholls, R. J., & Brown, S. (2018). Future response of global coastal wetlands to sea-level rise. *Nature*, *561*(7722), 231–234. https://doi.org/10.1038/s41586-018-0476-5

Smart, L. S., Taillie, P. J., Poulter, B., Vukomanovic, J., Singh, K. K., Swenson, J. J., Mitasova, H., Smith, J. W., & Meentemeyer, R. K. (2020). Aboveground carbon loss associated with the spread of ghost forests as sea levels rise. *Environmental Research Letters*, *15*(10), 104028. https://doi.org/10.1088/1748-9326/aba136

Smith, A. J., & Kirwan, M. L. (2021). Sea Level-Driven Marsh Migration Results in Rapid Net Loss of Carbon. *Geophysical Research Letters*, *48*(13), 1–11. https://doi.org/10.1029/2021GL092420

Smith, J. A. M. (2013). The Role of Phragmites australis in Mediating Inland Salt Marsh Migration in a Mid-Atlantic Estuary. *PLoS ONE*, *8*(5), e65091. https://doi.org/10.1371/journal.pone.0065091

St-Laurent, P., Friedrichs, M. A. M., Najjar, R. G., Shadwick, E. H., Tian, H., & Yao, Y. (2020). Relative impacts of global changes and regional watershed changes on the inorganic carbon balance of the Chesapeake Bay. *Biogeosciences*, *17*(14), 3779–3796. https://doi.org/10.5194/bg-17-3779-2020

Törnqvist, T. E., Cahoon, D. R., Morris, J. T., & Day, J. W. (2021). Coastal Wetland Resilience, Accelerated Sea-Level Rise, and the Importance of Timescale. *AGU Advances*, *2*(1). https://doi.org/10.1029/2020AV000334

Ury, E. A., Yang, X., Wright, J. P., & Bernhardt, E. S. (2021). Rapid deforestation of a coastal landscape driven by sea-level rise and extreme events. *Ecological Applications*, *31*(5), 1–11. https://doi.org/10.1002/eap.2339

Valentine, K., Herbert, E. R., Walters, D. C., Chen, Y., Smith, A. J., & Kirwan, M. L. (2023). Climate-driven tradeoffs between landscape connectivity and the maintenance of the coastal carbon sink. *Nature Communications*, *14*(1), 1137. https://doi.org/10.1038/s41467-023-36803-7

Walkinshaw, M., O'Geen, A., & Beaudette, D. (2022). *Soil Properties*. California Soil Resource Laborator. https://casoilresource.lawr.ucdavis.edu/soil-properties/

Walters, D. C., Carr, J. A., Hockaday, A., Jones, J. A., McFarland, E., Kovalenko, K. E., Kirwan, M. L., Cahoon, D. R., & Guntenspergen, G. R. (2021). Experimental Tree Mortality Does Not Induce Marsh Transgression in a Chesapeake Bay Low-Lying Coastal Forest. *Frontiers in Marine Science*, *8*. https://doi.org/10.3389/fmars.2021.782643

Ward, N. D., Megonigal, J. P., Bond-Lamberty, B., Bailey, V. L., Butman, D., Canuel, E. A., Diefenderfer, H., Ganju, N. K., Goñi, M. A., Graham, E. B., Hopkinson, C. S., Khangaonkar, T., Langley, J. A., McDowell, N.

G., Myers-Pigg, A. N., Neumann, R. B., Osburn, C. L., Price, R. M., Rowland, J., … Windham-Myers, L. (2020). Representing the function and sensitivity of coastal interfaces in Earth system models. *Nature Communications*, *11*(1), 2458. https://doi.org/10.1038/s41467-020-16236-2

Warnell, K., Olander, L., & Currin, C. (2022). Sea level rise drives carbon and habitat loss in the U.S. mid-Atlantic coastal zone. *PLOS Climate*, *1*(6), e0000044. https://doi.org/10.1371/journal.pclm.0000044

Wasson, K., Woolfolk, A., & Fresquez, C. (2013). Ecotones as Indicators of Changing Environmental Conditions: Rapid Migration of Salt Marsh–Upland Boundaries. *Estuaries and Coasts*, *36*(3), 654–664. https://doi.org/10.1007/s12237-013-9601-8

White, E. E., Ury, E. A., Bernhardt, E. S., & Yang, X. (2022). Climate Change Driving Widespread Loss of Coastal Forested Wetlands Throughout the North American Coastal Plain. *Ecosystems*, *25*(4), 812–827. https://doi.org/10.1007/s10021-021-00686-w

White, E., & Kaplan, D. (2021). Identifying the effects of chronic saltwater intrusion in coastal floodplain swamps using remote sensing. *Remote Sensing of Environment*, *258*(July 2020), 112385. https://doi.org/10.1016/j.rse.2021.112385

Williams, K., Ewel, K. C., Stumpf, R. P., Putz, F. E., & Workman, T. W. (1999). Sea-Level Rise and Coastal Forest Retreat on the West Coast of Florida, USA. *Ecology*, *80*(6), 2045. https://doi.org/10.2307/176677

Williams, K., Meads, M. V., & Sauerbrey, D. A. (1998). The roles of seedling salt tolerance and resprouting in forest zonation on thewest coast of Florida, USA. *American Journal of Botany*, *85*(12), 1745–1752. https://doi.org/10.2307/2446509